High-index-contrast, wide-FSR microring-resonator filter design and realization with frequency-shift compensation

Miloš A. Popović[†], Michael R. Watts[‡], Tymon Barwicz, Peter T. Rakich, Luciano Socci, Erich P. Ippen, Franz X. Kärtner and Henry I. Smith

Research Laboratory of Electronics, Massachusetts Institute of Technology, 77 Massachusetts Ave, Cambridge, Massachusetts 02139
[†]milos@mit.edu, [‡]mwatts@alum.mit.edu

Abstract: Rigorous electromagnetic simulations are used to design high-index-contrast microring-resonator filters. The first fabricated third-order filters compensated for passband distortion due to coupling-induced and fabrication-related frequency shifts demonstrate a 20nm FSR and the highest reported thru-port extinction (14dB).

OCIS codes: (130.3120) Integrated optics devices; (230.5750) Resonators; (230.7370) Waveguides.

1. Introduction

Coupled-microring filters are a promising approach to planar integrated-optical add/drop filters for wavelength-division multiplexed (WDM) networks [1-6]. Coupled cavities enable narrow, frequency-selective line-shapes with flat passbands while traveling-wave-cavity operation facilitates a natural separation of ports. Low-loss *drop-only* filters have been demonstrated [2-3] using microrings with a free spectral range (FSR) of ~ 6 nm. True *add/drop* filtering of a single WDM channel requires large resonator FSR spanning the optical band in use (~ 30 nm), and strong extinction of the dropped channel in the thru-port. Vernier schemes [4] can extend a small FSR, but tend to introduce intolerable dispersion into some thru channels. High index contrast (HIC) enhances confinement reducing bend loss in small-radius rings thereby enabling low-loss and wide-FSR filters directly [6]. Yet, HIC adds considerably to cavity design and fabrication challenges. Coupling-induced resonance frequency shifting (CIFS) [5,6] and excess losses due to coupler scattering [6] must be overcome in a successful design. Fabrication-related distortions of cavities (e.g. proximity effects) must also be countered. Detailed consideration of these issues and use of rigorous electromagnetic design, the importance of which we pointed to in [6], is yet absent in the literature.

We present design considerations for efficient HIC filters and rigorous analysis using three-dimensional, finite-difference cylindrical mode-solver and time-domain codes and experimental results on the first fabricated filters compensated for coupling-induced and fabrication-related cavity resonance shifts. The filters exhibit a 20 nm FSR and, as a result of the compensation, 14 dB in-band extinction in the thru-port, the highest reported result in third order microring filters. Measured results closely match the design response.

2. Design of HIC waveguides and resonators

The challenges in HIC design and fabrication are outlined through an example filter with a drop response having a flat-top, 40 GHz passband with ≥ 30 dB rejection 80 GHz from the passband center, and 20 dB extinction of the dropped channel across 40 GHz in the thru-port.

Differences in propagation and coupling strength between TE and TM modes make achieving polarization independence in HIC difficult. To do so, we design a single-polarization filter to be used within a balanced polarization-diversity scheme [7]. A wide, thin cross-section (Fig. 1a) waveguide was chosen. The geometry more tightly confines the intended TE mode, reduces the ring's sensitivities to sidewall roughness and its frequency dependence on waveguide width while providing a substantial mismatch between the propagation constants of the TE and TM modes. The mismatch inhibits crosstalk between the modes due to unintended perturbations by allowing the modes a chance to de-phase before substantial coupling takes place.

A 40-GHz filter corresponds roughly to an external Q of 4,000. For low filter losses a radiation Q ~ 100k is sought in the fundamental TE_{11} resonance. To analyze the ring modes, a full-vector cylindrical mode-solver is employed [9]. To arrive at a wide-FSR design, the ring radius is minimized while keeping the TE_{11} Q ~ 100k. The TM_{11} mode is also confined by the structure, but its presence is less of a concern since coupling to it is inhibited by the near-orthogonality of the cross-polarized modes in the coupling regions. However, the tight bend radii required to achieve large FSRs tend to re-confine modes that are cutoff in a straight guide, admitting spurious leaky resonances. The TE_{21} mode is of particular concern and must be suppressed, as it couples strongly to the TE_{11} mode in coupling regions resulting in excess loss [6]. The guide cross-section is adjusted to strongly suppress the undesired TE_{21} resonance. Qs of the TE_{11}, TM_{11} and TE_{21} resonances are shown in Fig. 1b. An 800x400 nm ring core with 100 nm overetch yields a 20 nm FSR and a Q ~ 90k for the TE_{11} resonance (order 52) at 1544.5 nm while

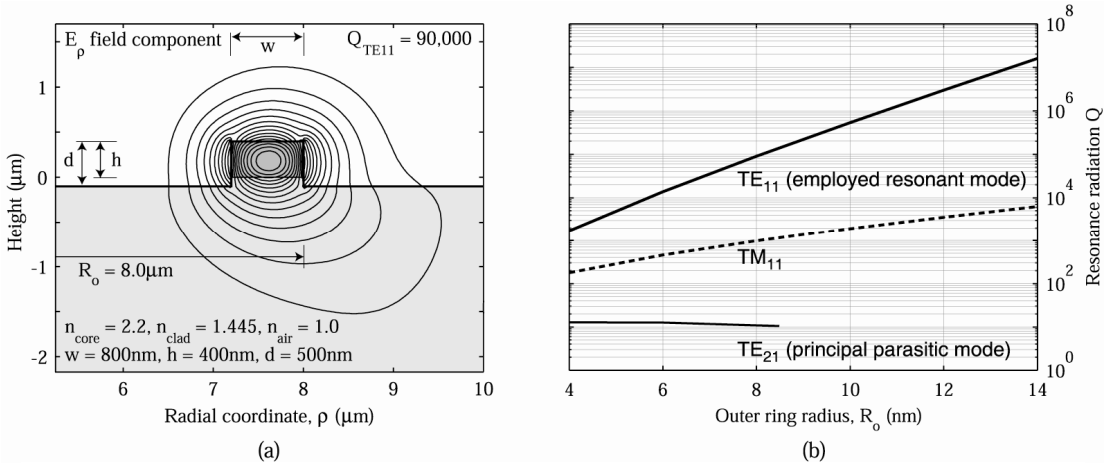

Fig. 1. (a) HIC ring waveguide cross-section with overlaid horizontal electric field pattern; (b) Q vs. radius and FSR for the fundamental TE_{11} and spurious TE_{21} and TM_{11} modes.

suppressing the TE_{21} and TM_{11} resonances to Qs of 10 and 980, respectively. Identical cross-sections were used for bus waveguides.

To synthesize the prescribed response, a third-order resonator requires 8.9 % ring-bus and 0.17 % ring-ring coupled power ratios. Complex coupling coefficients for various separations yield the power coupling, the excess cavity losses due to the interaction, and the coupling-induced resonance frequency shifts [5]. Rigorous 3D finite-difference time-domain (FDTD) simulations of the coupler regions were used to determine the complex ring-bus and ring-ring coupling coefficients at the resonant wavelength. The results, accompanied by exponential fits, are shown in Fig. 2. Rounded to a 6 nm scanning-electron-beam lithography (SEBL) system pixel size, 102 nm ring-bus and 492 nm ring-ring separations were chosen corresponding to the above couplings. With these separations the net CIFS in the outer rings is +38 GHz, which is comparable to the filter bandwidth. Clearly, the filter would not work without compensation of the frequency mismatch. The middle ring may be slightly pre-distorted in resonance frequency by the negative of the shift without changing appreciably any of the coupling parameters. An ideally compensated response shown in Fig. 3c (dash) gives a flat passband, 38 GHz 1dB bandwidth, 19 dB thru-port extinction, and 1.5 dB loss due to bending and coupler scattering.

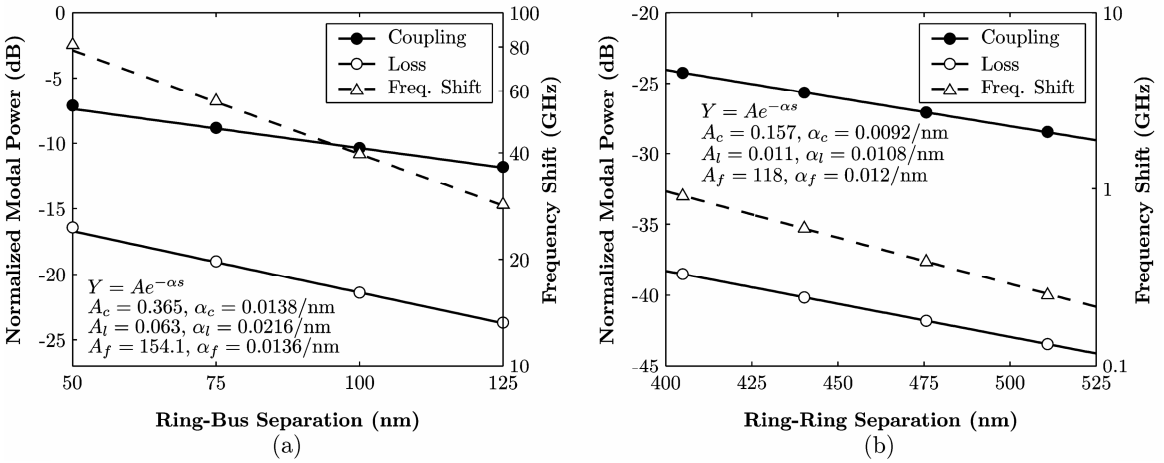

Fig. 2. 3D FDTD determined (a) Ring-Bus and (b) Ring-Ring, coupling, loss, and coupling-induced frequency shifts.

3. Fabrication and experimental results

The devices were fabricated using direct write SEBL. The fabrication process is similar to the one described in [7]. The pattern was defined in 200 nm of poly-methyl-methacrylate (PMMA) using a Raith 150 SEBL system at 30 keV. A hardmask was formed by evaporating and lifting off a thin film of Ni. The waveguides were created by a 500-nm-deep conventional reactive-ion etching step using a gas mixture of CHF_3 and O_2. Finally, the Ni hardmask

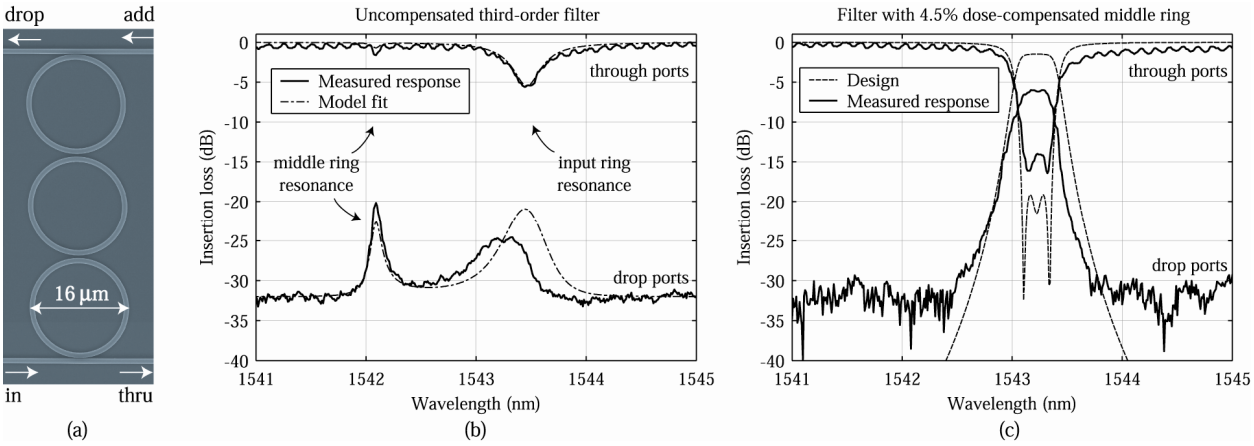

Fig. 3. (a) Micrograph of a compensated filter with 4.5% incremental dose applied to the middle ring; (b) drop- and thru-port responses of 3-ring filter without compensation – experiment (solid) and fit (dotted); (c) drop- and thru-port responses of compensated filter – theory (dash), theory with 15dB/cm waveguide loss (dotted) and experimental (solid).

was removed. The e-beam dose to the center ring of several identical filters was varied to slightly enlarge the center ring to tune it into resonance with the other rings in the filter. Fig. 3a is a micrograph of a fabricated filter.

Measured responses of the uncompensated and successfully compensated fabricated filters are shown in Figs. 3b and 3c. Care was taken to ensure that the drop- and thru-port responses have the same insertion loss scale. A fit to the uncompensated filter response indicated that the frequency of the center ring differed by 170 GHz from that of the rings adjacent to the bus waveguides. A 4.5% increase in the electron-beam dose to the center ring was required to compensate the frequency shift. The resulting compensated filter exhibits a 30 GHz-wide 1 dB passband in the drop port, with a rolloff that provides 25dB extinction 58 GHz from the channel center. In addition, a ~14 dB in-band rejection of the dropped channel in the thru-port was achieved, the highest reported for a high-order microring filter, and a crucial requirement for add/drop filters.

Higher than expected drop loss of 6dB rounds the compensated filter passband. Total ring loss was extracted by fitting the uncompensated response indicating an excess waveguide propagation loss of ~ 15 dB/cm. Accounting for this loss in the design model gives agreement with the measured filter response. The loss breakdown is 20 % due to bending, 20 % due to excess coupler scattering and 60 % attributed to roughness. The high propagation loss was also verified by the Fabry-Perot method using FDTD-computed facet reflectivity.

The higher than expected propagation loss is mainly attributed to an imperfect Ni liftoff. The Ni evaporation produced a thicker film (62 nm) than expected (45 nm) and a coarse microstructure, which amplified the line-edge-roughness of the Ni hardmask and translated to larger sidewall roughness and higher than expected scattering losses.

4. Conclusions

Rigorous electromagnetic analysis is needed for HIC filter design. Fabricated filters with proper compensation of coupling-induced and fabrication-related frequency mismatch in fabrication are shown necessary for successful realization of HIC microring filters with high extinction in the thru port. Dose compensation in e-beam fabrication was applied to demonstrate the first frequency-compensated filters, yielding 14dB extinction in the thru port, and matching design predictions.

References

1. J. V. Hryniewicz, P. P. Absil, B. E. Little, R. A. Wilson, and P.-T. Ho, "Higher order filter response in coupled microring resonators," IEEE Photon. Technol. Lett. Vol. 12, pp. 320-322, 2000.
2. B. E. Little, "A VLSI photonics platform," in *Optical Fiber Comm. Conf.* on CD-ROM (Optical Society of America, Washington, DC, 2004)
3. P. P. Absil, S. T. Chu, D. Gill, J. V. Hryniewicz, F. Johnson, O. King, B. E. Little, F. Seiferth and V. Van, "Very High Order Integrated Optical Filters" in *Optical Fiber Comm. Conf.* on CD-ROM (Optical Society of America, Washington, DC, 2004), TuL3.
4. Y. Yanagase, S. Suzuki, Y. Kokubun and S.T. Chu, "Box-like filter response and expansion of FSR by a vertically triple coupled microring resonator filter," J. Lightwave Technol. Vol. 20, 1525-1529 (2002).
5. C. Manolatou, M.A. Popović, P.T. Rakich, T. Barwicz, H.A. Haus and E.P. Ippen, "Spectral anomalies due to coupling-induced frequency shifts in coupled-resonator filters," in *Optical Fiber Comm. Conf.* on CD-ROM (Optical Society of America, Washington, DC, 2004), TuD5.
6. T. Barwicz, M. Popović, P.T. Rakich, M.R. Watts, H.A. Haus, E.P. Ippen and H.I. Smith, "Fabrication and analysis of add/drop filters based on microring resonators in SiN," in *Optical Fiber Comm. Conf. on CD-ROM* (Optical Society of America, Washington, DC, 2004), TuL4.
7. M. R. Watts, "Wavelength switching and routing through evanescently induced absorption," MS Thesis, Department of Electrical Engineering and Computer Science, Massachusetts Institute of Technology, Cambridge, MA, 2001.
8. M. Popović, "Complex-frequency leaky mode computations using PML boundary layers for dielectric resonant structures," in Integrated Photonics Research, OSA Technical Digest (Optical Society of America, Washington DC, 2003), pp. 143-145.